Underwater Optical Wireless Communications With InGaN LEDs Grown With an Asymmetric Multiple Quantum Well for Light Emission or Detection

Chia-Lung Tsai, Tong-Wen Wang, Ying-Chang Li, Atanu Das, Chia-Wei Chen, Yen-Jen Chen, and Sun-Chien Ko

***Abstract*—InGaN light-emitting diodes (LEDs) grown with an asymmetric multiple quantum well (MQW) are proposed for use in an optical link with an avalanche photodiode (APD) based receiver. In contrast to the high photoresponse of red AlGaInP LEDs in APDs, the proposed blue LEDs provide improved light output and enhanced system bandwidth for directed line-of-sight optical links passing through a 100-cm-long water tank. This improvement is due to the nonuniform carrier distribution within the InGaN MQWs being mitigated by using a thin GaN barrier near the n-GaN to facilitate hole transport capacity. In addition, bandwidth degradation resulting from APD module saturation can also be avoided by using these blue LEDs, successfully establishing a 300 Mbit/s LED-based underwater data link. The proposed InGaN LEDs (zero bias) under illumination exhibit a peak responsivity of 0.133 at $\lambda = 370$ nm, an ultraviolet (UV)-to-visible rejection ratio of 4849 and a 3-dB cut-off frequency of 33.3 MHz. Using violet UV laser diodes and the proposed LEDs respectively as the optical transmitter and receiver, an underwater optical link ($L = 100$ cm) with a data transmission rate of up to 130 Mbit/s and a bit error rate of 4.2×10^{-9} is also demonstrated.**

***Index Terms*—InGaN, light-emitting diodes, asymmetric multiple quantum well, photodiode, optical wireless communications.**

Manuscript received October 14, 2021; revised November 15, 2021; accepted November 20, 2021. Date of publication November 23, 2021; date of current version December 2, 2021. This work was financially supported in part by the Ministry of Science and Technology, Taiwan, under Grants MOST 110-2221-E-182-056-MY2, 110-2622-E-182-007, 108-2221-E-182-055, and MOST 107-2221-E-182-046, and in part by the Chang Gung Memorial Hospital, Linkou under Grants BMRP 999, CMRPD2K0201, and CMRPD2K0202. *(Corresponding author: Chia-Lung Tsai.)*

Chia-Lung Tsai is with the Department of Electronic Engineering and Green Technology Research Center, Chang Gung University, Taoyuan 33305, Taiwan, and also with the Department of Otolaryngology-Head and Neck Surgery, Chang Gung Memorial Hospital, Taoyuan 33305, Taiwan (e-mail: cltsai@mail.cgu.edu.tw).

Tong-Wen Wang is with the Department of Electronic Engineering, Feng Chia University, Taichung 40724, Taiwan (e-mail: tongwwang@fcu.edu.tw).

Ying-Chang Li is with the Green Technology Research Center, Chang Gung University, Taoyuan 33305, Taiwan (e-mail: davenlee15@gmail.com).

Atanu Das is with the Department of Pure and Applied Sciences, Midnapore City College, Midnapore, West Bengal 721129, India (e-mail: apu.atanu@outlook.com).

Chia-Wei Chen and Yen-Jen Chen are with the Department of Electronic Engineering, Chang Gung University, Taoyuan 33305, Taiwan (e-mail: wei26621907@gmail.com; sgamatha791219@gmail.com).

Sun-Chien Ko is with the Advanced Tech. Research Lab., Telecommunication Lab., Chunghwa Telecom Co., Ltd., Taoyuan 326402, Taiwan (e-mail: ko3838@cht.com.tw).

Digital Object Identifier 10.1109/JPHOT.2021.3130133

I. Introduction

ADVANCES in radio frequency (RF) based wireless communications allow for access to video-based multimedia through personal mobile devices, notebook computers, vehicles and so on. To fulfill demand for increased bandwidth and more efficient spectral usage, reduced latency and high reliability, 5G radio access networks have been proposed for use in a variety of applications such as massive machine communications or the Internet of Things (IoT) [1]. Aside from the development of millimeter-wave systems and advanced Wi-Fi technology [2], visible light-emitting diodes (LEDs) or laser diodes (LDs) have emerged as a promising optical transmitter for building an unlicensed, robust, and energy-efficient wireless communication systems [3], [4]. For LD-based optical wireless communications, despite the use of self-injection locked external cavity diode lasers (ECDL) [5], [6], the grating-coupled Littrow-type external cavity laser with its narrow spectral linewidth, flexible wavelength tenability, and high output power can also be used as an optical transmitter for high-speed data transmissions [7]–[9]. Another useful light source for such communication systems is based on the InGaN/GaN distributed feedback laser diode (DFB-LD). For these DFB LDs, further improvement in LD output performance (i.e., higher slope efficiency) can be achieved by using the sidewall gratings alongside the p-contact metal stripe on the ridge waveguide [10]. To attain high data transmission rates and allow for a degree of optical misalignment between the optical transmitter and the receiver, InGaN/GaN multiple-quantum-wells (MQW) LEDs are used in a directed line-of-sight optical link [11] even though their 3-dB modulation bandwidth (f_{3dB}) is lower than that of the LD transmitters. Further improvements to the system bandwidth of such optical links can be achieved by using surface plasmon coupling techniques (Ag-coated surface layer) to enhance the spontaneous emission rate and reduce the photon lifetime of InGaN LEDs [12]. Zhu *et al.* studied the impact of an AlGaN electron blocking layer (EBL) on the dynamic response of GaN-based LEDs, finding that a weak quantum-confined Stark effect and improved hole injection efficiency in InGaN MQWs can be achieved as the Al content of AlGaN EBLs is reduced from 20% to 15% [13]. Both factors are crucial for a high-speed InGaN LED. Alatawi *et al.* reported that the presence of the amplified spontaneous emission in edge-emitting blue LDs with a tilted output facet can help to boost their 3-dB bandwidth to a high value

($f_{3dB} > 400$ MHz) [14], allowing for the successful establishment of superluminescent diode-based optical links capable of 0.7 Gbit/s data transmissions with a bit error rate of 2.0×10^{-6} under a non-return-to-zero (NRZ) on-off keying (OOK) modulation scheme. Aside from the application of indoor/outdoor visible light communications, optical wireless communications with blue/green InGaN LEDs have advantages of low cost, high data rate, low latency and low power consumption, making such systems more suitable for use in underwater environments as compared to conventional underwater acoustic wave communications [15]. Shen *et al.* reported that the available data rate in a NRZ-OOK underwater optical link with a 450-nm LD and a Si avalanche photodetector (APD) is as high as 2 Gbit/s over a 12-m-long propagation distance and the corresponding bit error rate is measured to be 2.8×10^{-5} [16]. Despite using maximum ratio combination (MRC) receiving technology to improve the signal-to-noise ratio of the multi-PIN receiver, quadrature amplitude modulation (QAM)-discrete multitone (DMT) modulation is also proposed to realize a green InGaN LED-based underwater optical link (L = 1.2 m) capable of data transmission rates of 2.175 Gbit/s [17]. Lin *et al.* reported that high-speed underwater optical wireless communications (i.e., 660 Mbit/s data rate with a bit error rate of 3.3×10^{-3}) can be achieved using a green InGaN micro-LED transmitter [18]. In addition to functioning as a photovoltaic cell for underwater charging, 60 Mbit/s underwater optical communications with a bit error rate of 1.6×10^{-3} have also been performed using the same micro-LEDs as the photodetector (PD) and illuminated with a 450 nm blue LD.

For LED-based optical wireless communications, system performance is not only limited by the LED's 3-dB bandwidth but by the amount of the light available for collection at the receiver [19]. In general, this issue can be easily addressed by using a high-speed APD to increase the optical-to-electrical (OE) conversion efficiency at the receiving end, even though system performance may also be simultaneously affected by the amplified background signals [20]. Furthermore, AlGaInP LEDs should be better suited for use as optical transmitters due to the relatively high red-light photoresponse obtained in commercial APDs. In our previous work [21], we demonstrated that blue InGaN LEDs with asymmetric MQWs, in which a reduced layer thickness of GaN barriers close to n-GaN, provide enhanced light output power together with a higher 3-dB bandwidth. This makes the proposed InGaN LEDs the preferred light source for optical wireless communications as compared to that of their symmetric MQW counterparts. Using the proposed InGaN LEDs or commercial red AlGaInP LEDs as the optical transmitters, we experimentally investigate the influence of the LED characteristics on system performance of the APD receiver containing optical links passing through a 100-cm-long (tap) water tank. As a result of reduced carrier lifetimes or enhanced spontaneous emission rates in the proposed LEDs, the available 3-dB bandwidth and data transmission rate of InGaN LED-based underwater optical links outperform those obtained using AlGaInP LED transmitters. In addition to the presence of an apparent photoresponse under ultraviolet (UV) light illumination, a 3-dB cutoff frequency of 33.3 MHz is achieved in these PD-like InGaN LEDs biased at 0 V, allowing us to build an underwater optical link capable of 130 Mbit/s data transmission with a bit error rate of 4.2×10^{-9} using the proposed InGaN LEDs as the PD.

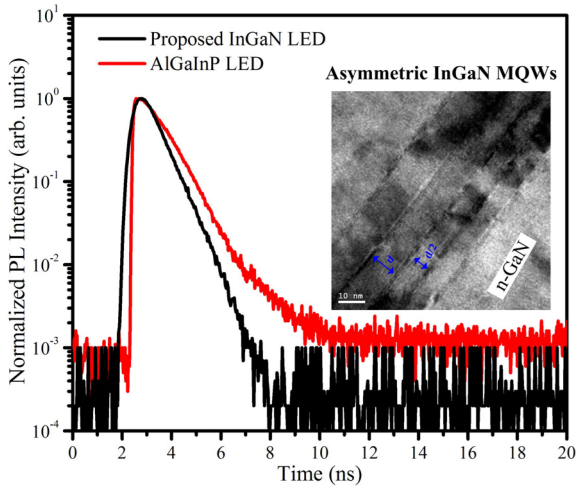

Fig. 1. TRPL spectrum measured at the PL peak position of the proposed InGaN LEDs and AlGaInP LEDs (i.e., the detection wavelength is respectively set at 436 nm and 628 nm for the blue and red LEDs). The inset shows the cross-sectional transmission electron microscope image of the proposed LEDs with asymmetric InGaN MQWs in which the GaN barriers near the n-GaN have a thickness half that of the others (d = 10 nm).

II. Experimental

Arima Optoelectronics Corp. produces AlGaInP LEDs with a chip size of 6.6 mil × 6.6 mil. The primary epistructure of red LED wafers grown on GaAs substrate is composed of a bottom distributed Bragg reflector (DBR), an AlGaInP MQW sandwiched between two AlInP cladding layers and a GaP window layer. The photon energy of red light is greater than the energy bandgap of the GaAs epilayer, thus the bottom DBRs reflect the downward-emitting photons towards the top surface to avoid substrate absorption [22]. On the other hand, as shown in Fig. 1, our proposed blue LEDs were grown with an asymmetric InGaN/GaN MQW in which GaN barriers near the n-GaN have a reduced layer thickness (d/2 = 5 nm) with respect to the others (d = 10 nm). For InGaN LEDs, the presence of nonuniform carrier distribution associated with low hole transport capacity is commonly observed in InGaN MQWs. This can cause significant optical deterioration during LED operations [23]. By introducing a thin GaN barrier near the n-GaN into the LED epistructure, the static and dynamic behaviors of the fabricated InGaN LEDs can be improved due to injected carriers (holes) penetrating deep into the quantum wells to participate in radiative recombinations [21]. After epitaxial growth, the InGaN LEDs were fabricated with a rectangular etched-mesa structure ($\sim$280 μm × 260 μm) for light emission.

For time-resolved photoluminescence (TRPL) measurements, the excitation light source is a 375 nm picosecond diode laser with an average optical power of 0.8 mW and a pulse width of 40 ps at a repetition rate of 8 MHz. The collected PL signal was analyzed using a time-correlated single-photon counting system with a temporal response of about 250 ps.

The light output performance of the TO-packaged LEDs without encapsulation and embedded in a metal heat sink was characterized by a Keithley Model 2400 source meter and a calibrated integrating optical sphere sensor (Newport Corp.). In addition to using a metal heat sink to facilitate heat dissipation, the TO-packaged LED was also soldered to a coaxial 50-Ω SMA microwave connector through a printed circuit board (PCB) for small- and large-signal analysis of the underwater optical links. The photoresponse and external quantum efficiency (EQE) of InGaN LEDs under illumination were measured by a detector responsivity measurement system (DSR100, Zolix) with a 75-W tungsten halogen lamp, monochromator, chopper and a lock-in amplifier. Prior to testing, pre-calibration was performed using a standard Si PD (DSR-A1, Zolix).

III. Results and Discussion

Fig. 1 shows the TRPL spectrum measured at the photoluminescence (PL) peak position of the proposed InGaN LEDs and AlGaInP LEDs. The lifetimes of the photogenerated carriers in the proposed InGaN LED and AlGaInP LED are respectively estimated as 649 ps and 972 ps through the numerical fitting of the TRPL results with a single-exponential decaying function [12]. For InGaN LEDs, the tilted potential profile of InGaN MQWs is due to the polarization-induced electric fields in GaN-based semiconductors [24], leading to reduced oscillator strength and longer carrier lifetimes in these LEDs. However, the absence of polarization fields in AlGaInP LEDs [25] should result in shorter carrier lifetimes compared to the proposed InGaN LEDs. This is contrary to the finding from the TRPL measurement. Therefore, we speculate that highly efficient radiation and/or improved frequency response could be achieved in our proposed LEDs grown with an asymmetric InGaN MQW. To verify this, further experiments were conducted to investigate their static and dynamic behaviors.

Considering effective light output power (without shielding from the metal electrodes) and LED chip size, Fig. 2 shows the available light output of the LEDs operating at different current densities. The forward voltage (@ 20 mA) and the equivalent series resistance evaluated from the forward current versus voltage (I-V) characteristics of the proposed InGaN LEDs and AlGaInP LEDs are respectively 2.98 V and 6.9 Ω, and 1.96 V and 2.3 Ω. In addition, ideality factors of 4.3 and 1.8 are respectively found for the proposed LEDs and AlGaInP LEDs. Because our InGaN LEDs were grown on lattice-mismatched sapphire substrates, the distinct misfit-induced defects (i.e., threading dislocation density $\sim 5.8 \times 10^8$ cm^{-2} from X-ray diffraction analysis) result in a higher ideality factor as compared to that of AlGaInP LEDs. The anomalous red-blue-red peak shifts in the temperature-dependent PL spectrum of the proposed InGaN LEDs (not shown here) clearly suggest the formation of indium-rich nanoclusters in InGaN wells [26]. This will help injection carriers radiatively recombine at localized states instead of being captured by nonradiative recombination centers [27]. Furthermore, a thin GaN barrier near the n-GaN was proposed to mitigate nonuniform carrier distribution within the InGaN MQWs and to facilitate radiative recombinations [21].

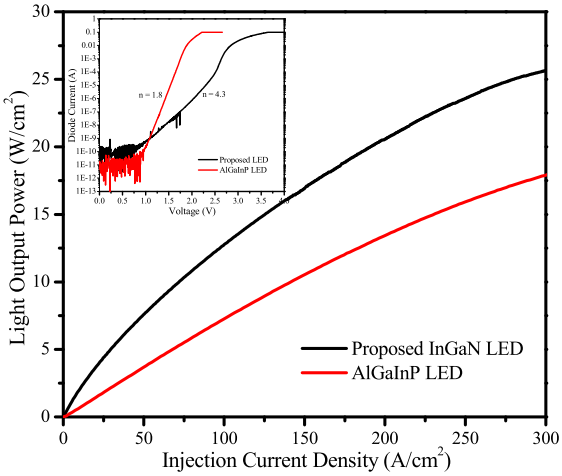

Fig. 2. Dependency of injection current density on the effective light output power (without shielding from the metal electrodes) of the proposed InGaN LED and AlGaInP LED. The inset shows the corresponding I-V characteristics of the LEDs.

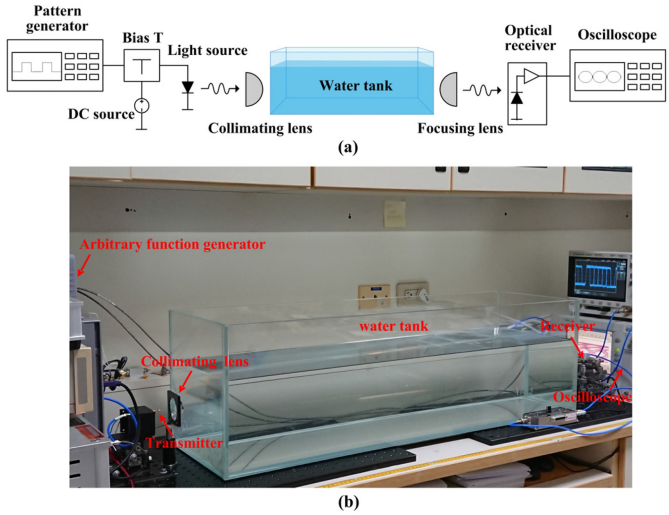

Fig. 3. (a) Schematic diagram of the experimental setup for transmission of digital signals through a 100-cm-long water (tap water) tank using an optical link with the LED transmitter and the APD receiver. (b) Photograph of directed line-of-sight LED-based underwater optical links.

Consequently, a 1.4 times (@ J = 300 A/cm^2) increase in light output power is achieved in the proposed InGaN LEDs despite their material defects. This is consistent with the result given from the TRPL measurement.

Fig. 3 shows the experimental setup used to transmit digital signals through a 100-cm-long water (tap water) tank using an optical link with the LED transmitter and the APD receiver. For large-signals analysis of an underwater optical link [28], the nonreturn-to-zero (NRZ) pseudorandom bit sequence (PRBS) signals from the arbitrary function generator (Agilent 81160A) are combined with the bias current (I_{Bias}) through a bias tee (ZX85-12G, Mini-Circuits) and then fed to the TO-packaged LEDs. A plano-convex lens (collimating lens) placed in front of the optical transmitter is used to form a directed light beam towards the receiver. At the receiving end, we use another

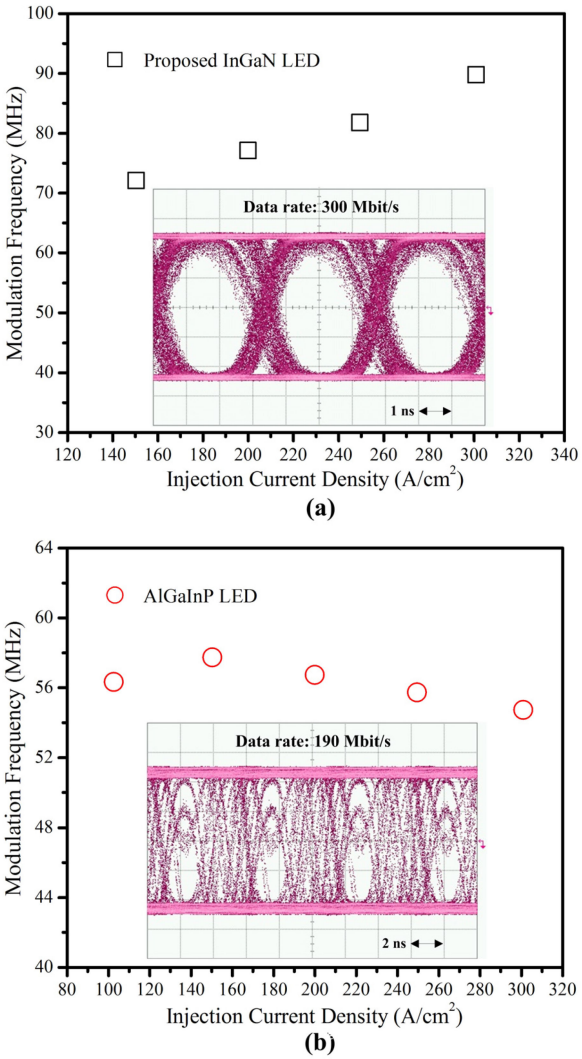

Fig. 4. System bandwidth as a function of injection current density of (a) the proposed InGaN LED transmitter and (b) AlGaInP LED transmitter for the direct line-of-sight optical link passing through a 100-cm-long water tank. For the InGaN LED (AlGaInP LED) based optical links, the eye diagram measured at 300 Mbit/s (190 Mbit/s) corresponding to the system bandwidth of 89.7 MHz (57.7 MHz) is also shown. During the large-signal measurements, the InGaN LED and AlGaInP LED were respectively operating at J = 301.2 A/cm^2 and 150.6 A/cm^2. In addition, the V_{PP} and the word lengths of the NRZ PRBS signals were set as 5 V and 2^7-1.

plano-convex lens to facilitate propagation light collection by a high-speed APD (AD500-9-400M-TO5, Pacific). Finally, the amplified electrical signal was analyzed by a wide-bandwidth sampling oscilloscope (Agilent 86100A). In this optical link, the light coupling efficiency between the transmitter and the receiver is estimated at 23.7%. Using visible LEDs as the optical transmitter, the system bandwidth of an underwater optical link measured using a vector network analyzer (Rohde & Schwarz ZVL-13) is shown in Fig. 4. The system bandwidth of AlGaInP LED based optical links initially increases with the injection current density (i.e., f_{3dB} = 56.3 MHz and 57.7 MHz at 102.9 A/cm^2 and 150.6 A/cm^2) and then gradually falls to 54.7 MHz at elevated current levels (J = 301.2 A/cm^2). A higher spectral responsivity (relative to blue light) is presented in the used APDs

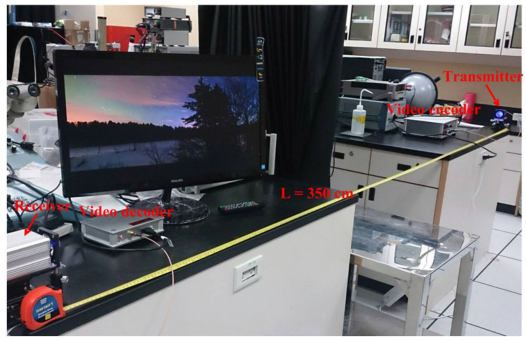

Fig. 5. Experimental setup of a free-space optical link used for transmission of digital video signals at a 350-cm-long propagation distance.

illuminated with red light, thus the APD module saturation is seen as causing the bandwidth degradation observed at higher currents [20] despite the relatively low output power of AlGaInP LEDs compared to InGaN LEDs. As a result of reduced carrier lifetimes or enhanced spontaneous emission rates [29], system bandwidth is observed to increase monotonically with current using the proposed InGaN LED transmitters. In this underwater optical link, the maximum system bandwidth of 89.7 MHz achieved at J = 301.2 A/cm^2 is higher than that obtained using AlGaInP LEDs (f_{3dB} = 57.7 MHz at J = 150.6 A/cm^2). It is worth noting that, even for the same injection current density (J ~150 A/cm^2), a higher bandwidth is still found in the InGaN LED based optical links (i.e., f_{3dB} = 72 MHz versus 57.7 MHz). As evaluated from the electroluminescence (EL) spectrum (not shown here) of the proposed InGaN LEDs and AlGaInP LEDs operating at different current densities, both LEDs exhibit a temperature-induced redshift of the EL peak position as the injection current density increased from 50 A/cm^2 to 300 A/cm^2. For the proposed InGaN LEDs, the redshift rate is 0.014 nm per A/cm^2 (i.e., the emission wavelength redshifted from 444.4 nm to 447.9 nm) while a similar redshift rate of 0.018 nm per A/cm^2 was found in the AlGaInP LEDs. These results suggest that the lower 3-dB bandwidth of an underwater optical link with the AlGaInP LEDs does not result from their poor thermal performance at high current levels. The improved system bandwidth of an underwater optical link with the proposed InGaN LEDs provides data transmission of 300 Mbit/s with a clear and open eye pattern measured at 300 Mbit/s (inset of Fig. 4(a)). The rise time, fall time and the peak-to-peak jitter are respectively 1.2 ns, 1.2 ns and 511 ps. In contrast, no well-resolved eye pattern is observed in the AlGaInP LED based optical links (due to insufficient system bandwidth) even for a lower data rate of 190 Mbit/s. During the large-signal measurements, the InGaN LED and AlGaInP LEDs respectively operated at J = 301.2 A/cm^2 and 150.6 A/cm^2. In addition, the peak-to-peak voltage (V_{PP}) and the word length of NRZ PRBS signals were respectively set as 5 V and $2^7 - 1$. Instead of using a water tank with restricted dimensions to build an underwater optical link, optical wireless communications in free space were also performed. Fig. 5 shows the experimental setup of a free-space optical link used for the transmission of digital video signals. In the transmitting terminals, computer-readable recording media such MPEG video files were processed

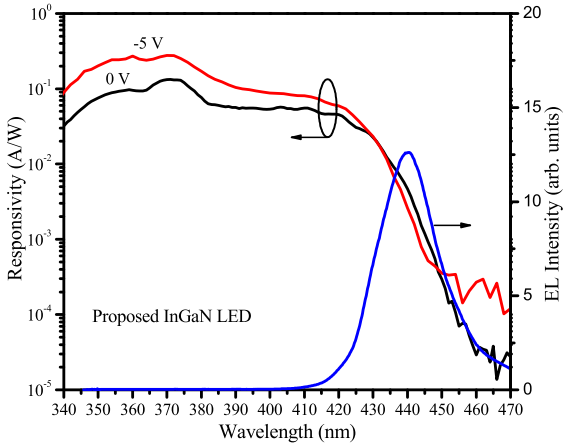

Fig. 6. The spectral responsivity of the proposed InGaN LEDs (biased at 0 V and −5 V) under illumination. The inset shows the EL spectrum of the proposed InGaN LEDs operating at I = 10 mA.

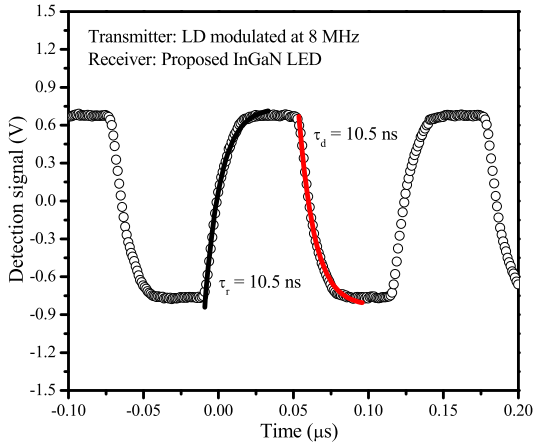

Fig. 7. Transient response of the proposed InGaN LED (zero bias) illuminated by a commercial violet UV LD with a modulation frequency (square wave) of 8 MHz.

using a commercial MPEG decoder (SmartMPEG-M, Fujitsu) to generate the digital video signals. Then, a field programmable gate array (FPGA) implementation of the video encoder (MAX 10 10M08SAE144C8G, Intel) was used to generate a serial video signal, which is fed to the proposed InGaN LEDs (I_{Bias} = 150 mA) to generate the modulated light. At the receiving end, an optical detector (AD500-9-400M-TO5, Pacific) and a video decoder (MAX 10 10M08SAE144C8G, Intel) were used to recover the original video signals which were then displayed on a monitor. As shown in Fig. 5, when a direct line-of-sight optical link (data rate ∼250 Mbit/s) is established between the LED transmitter and the APD receiver, the video image can be clearly observed on the monitor even at a long light propagation distance (L = 350 cm). System performance for optical wireless communications can be further improved by shrinking the LED size to increase their 3-dB modulation bandwidth [18], [30] or by using an advanced modulation scheme such as QAM-DMT modulation [17], orthogonal frequency division multiplexing [31] or four-level pulse amplitude modulations [32], [33] to enhance the data rate.

Apart from functioning as optical transmitters to provide data connectivity, the photoresponse of the proposed InGaN LEDs under illumination was examined to verify their capacity for use as a PD. Fig. 6 shows the spectral responsivity of the proposed InGaN LEDs (biased at 0 V and −5 V) under illumination, along with the EL spectrum of InGaN LEDs operating at I = 10 mA. The PD-like InGaN LEDs at zero bias exhibit a wavelength-dependent photoresponse with a peak responsivity of 0.133 A/W or an external quantum efficiency of 44.3% at λ = 370 nm. As shown in Fig. 6, the photoresponse of the PD-like InGaN LEDs can be further improved by increasing the reverse DC bias from 0 V to −5 V. However, this will suffer from the increased responsivity (or increased noise level) at longer wavelengths (λ > 450 nm) due to increased leakage current (or dark current) of InGaN PDs operating at a higher negative voltage [34]. As a result of the quantum-confined Franz-Keldysh effect and indium compositional inhomogeneity in InGaN MQWs [35], the InGaN-related absorption process covers a wide range of energy transitions so that a gradually increased responsivity is observed in the wavelength range of 420 nm to 470 nm. In addition, the observation of the spectral overlap between the EL emission and detection spectrum indicates bidirectional optical wireless communications might be performed with two proposed InGaN LEDs rather than using an additional PD for light detection [36]. Furthermore, the rejection ratio of the photoresponse in UV relative to visible light (defined as the photoresponsivity at λ = 370 nm relative to that obtained at λ = 470 nm) reaches 4849, indicating that good wavelength selectivity can be achieved in these PD-like InGaN LEDs at zero bias. In addition, the normalized detectivity (D^*) of the PDs can also be determined by $D^* = R_\lambda/(2qJ_d)^{1/2}$ [37], where R_λ is the responsivity, J_d is the dark current density of the detector and q is the electron charge (1.6×10^{-19} C). For the proposed InGaN LEDs under illumination, the peak D^* is calculated to be 5.5×10^{11} cm $Hz^{1/2}W^{-1}$ at zero bias, comparable to that of the Schottky-type GaN PDs [37]. For the InGaN MQW PDs, the PD's output performance is affected by its epistructure design features such as the number of quantum wells, and the layer thickness and doping level of GaN barriers and AlGaN electron block layer [38]. Therefore, further optimizing the InGaN LED structure is necessary as they were used as the optical transmitter or receiver.

Fig. 7 shows the transient response of proposed InGaN LEDs (zero bias) illuminated by a commercial violet UV LD (λ = 405 nm & $f_{3dB} \sim 1$ GHz) with a modulation frequency (square wave) of 8 MHz. During measurements, the LD was pre-biased at 35 mA with V_{PP} = 1 V. The optical link used is similar to that shown in Fig. 3 except that the light propagation distance is reduced to 10 cm in free space. At the receiving end, after the OE conversion by the PD-like InGaN LED, the electrical signal was amplified by a 44 dB amplifier (DHPCA-100, FEMTO Messtechnik GmbH) and then displayed using a digital oscilloscope (DSO-X 3034A, Agilent). As shown in Fig. 7, the distinct high (low) level of the detection signals corresponds to the intense (weak) light output of the LDs modulated at 8 MHz. The rise time (τ_r) and fall time (τ_d) can be given by curve fitting

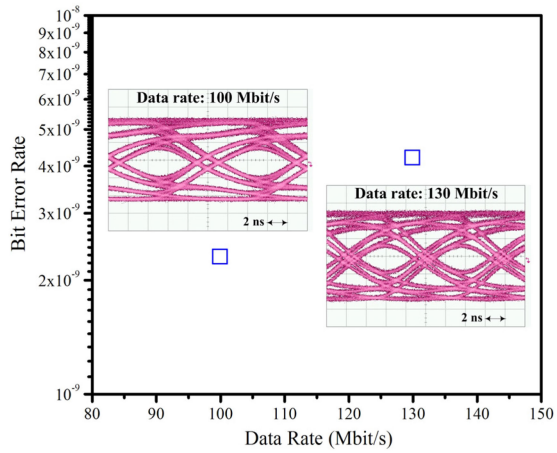

Fig. 8. Bit error rate of a 100 (130) Mbit/s optical link passing through a 100-cm-long water tank. The violet UV LD and PD-like InGaN LED were respectively used as the optical transmitter and receiver. During measurements, the LD was pre-biased at 30 mA with $V_{PP} = 1.5$ V. In addition, the bias voltage of the InGaN LEDs is set at 0 V and −5 V with respective data rates of 100 Mbit/s and 130 Mbit/s. The corresponding eye diagrams measured at 100 Mbit/s and 130 Mbit/s (word length $= 2^7 - 1$) are also shown.

of the experimental data using the following equations [39]:

$$V = V_0 \left[1 - \exp\left(-\frac{t}{\tau_r}\right)\right] \quad (1)$$

$$V = V_0 \exp\left(-\frac{t}{\tau_d}\right) \quad (2)$$

where V_0 is the maximum photovoltage at a particular time t. The τ_r and τ_d are both found to be 10.5 ns. Therefore, the maximum 3-dB cut-off frequency of the proposed InGaN LEDs (zero bias) under modulated light detection can be estimated at 33.3 MHz [40].

Using the violet UV LD ($\lambda = 405$ nm) and the proposed InGaN LED respectively as the optical transmitter and receiver, the system performance of the direct optical links passing through a 100-cm-long water tank is investigated by using a bit error rate tester (Agilent E4861B). The relevant results are summarized in Fig. 8. During measurements, the LD was pre-biased at 30 mA with $V_{PP} = 1.5$ V. In addition, the bias voltage of the PD-like InGaN LEDs with a 44 dB amplifier is respectively set at 0 V and −5 V for data rates of 100 Mbit/s and 130 Mbit/s. The corresponding eye diagrams measured at 100 Mbit/s and 130 Mbit/s (word length $= 2^7$-1) are also shown. Underwater optical links using the PD-like InGaN LEDs at zero bias are found to be capable of 100 Mbit/s data transmission with a bit error rate of 2.3×10^{-9}, which is also reflected in the good eye pattern quality. Further reducing the PD's bias to −5 V improves the data transmission rate to 130 Mbit/s, though with a slightly degraded bit error rate ($\sim 4.2 \times 10^{-9}$). In addition to a low junction capacitance caused by the wider depletion layer, the photocurrent can also be generated through the avalanche multiplication within the *pn* junction with an intense electrical field as the reverse bias voltage was increased [41]. Both factors are considered responsible for the improved transmission performance (i.e., higher data rate) of the proposed underwater optical links with the PD-like InGaN LEDs biased at −5 V. It should be noted that, when the LD emitter is replaced by the proposed InGaN LED (i.e., LED-LED optical links), the light divergence property of the emitter reduces the available data rate to 35 Mbit/s even though the separation distance between the transmitter and the receiver is reduced to 10 cm in free space. In this LED-LED optical link with a directional beam, the light coupling efficiency is only about 37% relative to that obtained using the LD emitter ($\eta = 60.8\%$) at a propagation distance of 100 cm in tap water (Fig. 3).

IV. Conclusion

The improved output performance of blue InGaN LEDs makes them better suited for use in an APD receiver containing optical link passing through a 100-cm-long water tank. This is due to a thin GaN barrier near the n-GaN facilitating uniform carrier distribution within the InGaN MQWs of the proposed blue LEDs. In addition, the formation of indium-rich nanoclusters in InGaN also alleviates defect-induced nonradiative recombinations. Therefore, a higher light output power can be achieved in the proposed InGaN LEDs as compared to commercial red AlGaInP LEDs, consistent with the TRPL result. Using the proposed InGaN LED as an optical transmitter improves the system bandwidth of the APD receiver containing optical links passing through a tap water tank (L = 100 cm) (i.e., $f_{3dB} =$ 89.7 MHz at J = 301.2 A/cm^2) despite the APDs having a low blue-light photoresponse. This allows for 300 Mbit/s data transmission through such underwater optical links. On the other hand, the proposed InGaN LEDs (zero bias) also exhibit a UV light photoresponse with a peak responsivity of 0.133 A/W at $\lambda = 370$ nm, a UV-to-visible rejection ratio of 4849 and a 3-dB cut-off frequency of 33.3 MHz. Finally, we demonstrate an underwater optical link (L = 100 cm) with data transmission rates of up to 130 Mbit/s with a bit error rate of 4.2×10^{-9} respectively using violet UV LDs and the proposed InGaN LEDs as the optical transmitter and receiver.

References

[1] Y. P. E. Wang *et al.*, "A primer on 3GPP narrowband internet of things," *IEEE Commun. Mag.*, vol. 55, no. 3, pp. 117–123, Mar. 2017, doi: 10.1109/MCOM.2017.1600510CM.

[2] E. J. Oughton, W. Lehr, K. Katsaros, I. Selinis, D. Bubley, and J. Kusum, "Revisiting wireless internet connectivity: 5G vs Wi-Fi 6," *Telecommun. Policy*, vol. 45, no. 5, Mar. 2021, Art. no. 102127, doi: 10.1016/j.telpol.2021.102127.

[3] T. Taki and M. Strassburg, "Visible LEDs: More than efficient light," *ECS J. Solid State Sci. Technol.*, vol. 9, Nov. 2020, Art. no. 015017, doi: 10.1149/2.0402001JSS.

[4] F. Zafar, M. Bakaul, and R. Parthiban, "Laser-diode-based visible light communication: Toward gigabit class communication," *IEEE Commun. Mag.*, vol. 55, no. 2, pp. 144–151, Feb. 2017, doi: 10.1109/MCOM.2017.1500672CM.

[5] S. Mukhtar, X. Sun, I. Ashry, T. K. Ng, B. S. Ooi, and M. Z. M. Khan, "Tunable violet laser diode system for optical wireless communication," *IEEE Photon. Technol. Lett.*, vol. 32, no. 9, pp. 546–549, May 2020, doi: 10.1109/LPT.2020.2983548.

[6] M. H. M. Shamim *et al.*, "Analysis of optical injection on red and blue laser diodes for high bit-rate visible light communication," *Opt. Commun.*, vol. 449, pp. 79–85, May 2019, doi: 10.1016/j.optcom.2019.05.034.

[7] D. Ding, X. Lv, X. Chen, F. Wang, J. Zhang, and K. Che, "Tunable high-power blue external cavity semiconductor laser," *Opt. Laser Technol.*, vol. 94, pp. 1–5, Mar. 2017, doi: 10.1016/j.optlastec.2017.03.015.

[8] D. Ding *et al.*, "Influence of grating parameters on the performance of a high-power blue external-cavity semiconductor laser," *Appl. Opt.*, vol. 57, no. 7, pp. 1589–1593, Mar. 2018, doi: 10.1364/AO.57.001589.

[9] M. H. Chen, S. C. Hsiao, K. T. Shen, C. C. Tsai, and H. C. Chui, "Single longitudinal mode external cavity blue InGaN diode laser," *Opt. Laser Technol.*, vol. 116, pp. 68–71, Aug. 2019, doi: 10.1016/j.optlastec.2019.03.022.

[10] Z. Deng, J. Li, M. Liao, W. Xie, and S. Luo, "InGaN/GaN distributed feedback laser diodes with surface gratings and sidewall gratings," *Micromachines*, vol. 10, no. 10, Oct. 2019, Art. no. 699, doi: 10.3390/mi10100699.

[11] L. Grobe *et al.*, "High-speed visible light communication systems," *IEEE Commun. Mag.*, vol. 51, no. 11, pp. 60–66, Dec. 2013, doi: 10.1109/MCOM.2013.6685758.

[12] K. Okamoto, I. Niki, A. Scherer, Y. Narukawa, T. Mukai, and Y. Kawakami, "Surface plasmon enhanced spontaneous emission rate of InGaN/GaN quantum wells probed by time-resolved photoluminescence spectroscopy," *Appl. Phys. Lett.*, vol. 87, no. 7, Aug. 2005, Art. no. 071102, doi: 10.1063/1.2010602.

[13] S. Zhu *et al.*, "Influence of AlGaN electron blocking layer on modulation bandwidth of gan-based light emitting diodes," *ECS Solid State Lett.*, vol. 3, no. 3, pp. R11–R13, Jan. 2014, doi: 10.1149/2.007403ssl.

[14] A. A. Alatawi *et al.*, "High-power blue superluminescent diode for high CRI lighting and high-speed visible light communication," *Opt. Exp.*, vol. 26, no. 20, pp. 26355–26364, Oct. 2018, doi: 10.1364/OE.26.026355.

[15] H. Kaushal and G. Kaddoum, "Underwater optical wireless communication," *IEEE Access*, vol. 4, pp. 1518–1547, 2016, doi: 10.1109/ACCESS.2016.2552538.

[16] C. Shen *et al.*, "20-meter underwater wireless optical communication link with 1.5 Gbps data rate," *Opt. Exp.*, vol. 24, no. 22, pp. 25502–25509, Oct. 2016, doi: 10.1364/OE.24.025502.

[17] F. Wang, Y. Liu, F. Jiang, and N. Chi, "High speed underwater visible light communication system based on LED employing maximum ratio combination with multi-PIN reception," *Opt. Commun.*, vol. 425, pp. 106–112, Oct. 2018, doi: 10.1016/j.optcom.2018.04.073.

[18] R. Lin, X. Liu, G. Zhou, Z. Qian, X. Cui, and P. Tian, "InGaN micro-LED array enabled advanced underwater wireless optical communication and underwater charging," *Adv. Opt. Mater.*, vol. 9, no. 12, Apr. 2021, Art. no. 2002211, doi: 10.1002/adom.202002211.

[19] H. Li, X. Chen, J. Guo, and H. Chen, "A 550 Mbit/s real-time visible light communication system based on phosphorescent white light LED for practical high-speed low-complexity application," *Opt. Exp.*, vol. 22, no. 22, pp. 27203–27213, Nov. 2014, doi: 10.1364/OE.22.027203.

[20] M. Gao, C. Li, and Z. Xu, "Optimal transmission of VLC system in the presence of LED nonlinearity and APD module saturation," *IEEE Photon. J.*, vol. 10, no. 5, Sep. 2018, Art. no. 7907514, doi: 10.1109/JPHOT.2018.2871148.

[21] C. L. Tsai and Y. J. Chen, "Real-time optical wireless transmissions of digital TV signals using white InGaN LEDs grown with an asymmetric quantum barrier," *Opt. Exp.,* vol. 23, no. 21, pp. 28059–28066, Oct. 2015, doi: 10.1364/OE.23.028059.

[22] H. J. Lee *et al.*, "Efficiency improvement of 630 nm AlGaInP light-emitting diodes based on Algaas bottom window," *Jpn. J. Appl. Phys.*, vol. 52, Sep. 2013, Art. no. 102101, doi: 10.7567/JJAP.52.102101.

[23] Ü. Özgür, H. Liu, X. Li, X. Ni, and H. Morkoç, "GaN-based light-emitting diodes: Efficiency at high injection levels," *Proc. IEEE*, vol. 98, no. 7, pp. 1180–1196, Jul. 2010, doi: 10.1109/JPROC.2010.2043210.

[24] J. H. Ryou *et al.*, "Control of quantum-confined stark effect in ingan-based quantum wells," *IEEE J. Sel. Top. Quantum Electron.*, vol. 15, no. 4, pp. 1080–1091, Jul./Aug. 2009, doi: 10.1109/JSTQE.2009.2014170.

[25] J. I. Shim *et al.*, "Efficiency droop in AlGaInP and GaInN light-emitting diodes," *Appl. Phys. Lett.*, vol. 100, no. 11, Mar. 2012, Art. no. 111106, doi: 10.1063/1.3694044.

[26] Y. H. Cho *et al.*, "'S-shaped' temperature-dependent emission shift and carrier dynamics in InGaN/GaN multiple quantum wells," *Appl. Phys. Lett.*, vol. 73, no. 10, pp. 1370–1372, Sep. 1998, doi: 10.1063/1.122164.

[27] J. Bai, T. Wang, and S. Sakai, "Influence of the quantum-well thickness on the radiative recombination of InGaN/GaN quantum well structures," *J. Appl. Phys.*, vol. 88, no. 8, pp. 4729–4733, Oct. 2000, doi: 10.1063/1.1311831.

[28] R. Windisch *et al.*, "Large-signal-modulation of high-efficiency light-emitting diodes for optical communication," *IEEE J. Quantum Electron.*, vol. 36, no. 12, pp. 1445–1453, Dec. 2000, doi: 10.1109/3.892565.

[29] J. J. D. McKendry *et al.*, "Visible-light communications using a CMOS-controlled micro-light-emitting-diode array," *J. Lightw. Technol.*, vol. 30, no. 1, pp. 61–67, Jan. 2012, doi: 10.1109/JLT.2011.2175090.

[30] P. P. Maaskant *et al.*, "High-speed substrate-emitting micro-light-emitting diodes for applications requiring high radiance," *Appl. Phys. Exp.*, vol. 6, no. 2, Feb. 2013, Art. no. 022102, doi: 10.7567/APEX.6.022102.

[31] M. S. Islim *et al.*, "Towards 10 Gb/s orthogonal frequency division multiplexing-based visible light communication using a GaN violet micro-LED," *Photon. Res.*, vol. 5, no. 2, pp. A35–A43, Apr. 2017, doi: 10.1364/PRJ.5.000A35.

[32] C. Y. Li *et al.*, "16 Gb/s PAM4 UWOC system based on 488-nm LD with light injection and optoelectronic feedback techniques," *Opt. Exp.*, vol. 25, no. 10, pp. 11598–11605, May 2017, doi: 10.1364/OE.25.011598.

[33] H. H. Lu *et al.*, "A 56 Gb/s PAM4 VCSEL-based LiFi transmission with two-stage injection-locked technique," *IEEE Photon. J.*, vol. 9, no. 1, Feb. 2017, Art. no. 7900208, doi: 10.1109/JPHOT.2016.2637564.

[34] K. T. Ho *et al.*, "3.2 gigabit-per-second visible light communication link with InGaN/GaN MQW micro-photodetector," *Opt. Exp.*, vol. 26, no. 3, pp. 3037–3045, Feb. 2018, doi: 10.1364/OE.26.003037.

[35] Y. Zhang *et al.*, "Stokes shift in semi-polar (11-22) InGaN/GaN multiple quantum wells," *Appl. Phys. Lett.*, vol. 108, no. 3, Jan. 2016, Art. no. 031108, doi: 10.1063/1.4940396.

[36] Y. Wang, F. Wu, X. Wang, and J. Yuan, "GaN photonics: Simultaneous emission-detection phenomenon of multiple quantum well diode," *Proc. SPIE, Nanophotonics and Micro/Nano Opt. IV*, vol. 10823, Oct. 2018, Art. no. 108230H, doi: 10.1117/12.2503132.

[37] B. Ren *et al.*, "Vertical-type Ni/GaN UV photodetectors fabricated on free-standing GaN substrates," *Appl. Sci.*, vol. 9, Jul. 2019, Art. no. 2895, doi: 10.3390/app9142895.

[38] J. Pereiro *et al.*, "Optimization of InGaN–GaN MQW photodetector structures for high-responsivity performance," *IEEE J. Quantum Electron.*, vol. 45, no. 6, pp. 617–622, Jun. 2009, doi: 10.1109/JQE.2009.2013140.

[39] C. L. Tsai, T. W. Wang, Y. C. Lu, A. Das, S. H. Chang, and S. C. Ko, "Fabrication and characterization of dual functional InGaN LED arrays as the optical transmitter and receiver for optical wireless communications," *IEEE Photon. J.*, vol. 13, no. 2, Apr. 2021, Art. no. 8200311, doi: 10.1109/JPHOT.2021.3069841.

[40] D. Decoster and J. Harari, *Optoelectronic Sensors*. Hoboken, NJ, USA: Wiley, 2009, ch. 1, ISBN: 978-1-848-21078-3.

[41] M. Kowalczyk and J. Siuzdak, "Photo-reception properties of common LEDs," *Opto-Electron. Rev.*, vol. 25, no. 3, pp. 222–228, Sep. 2017, doi: 10.1016/j.opelre.2017.06.009.